

Structures and topological transitions of hydrocarbon films on quasicrystalline surfaces

Wahyu Setyawan¹, Renee D. Diehl², and Stefano Curtarolo^{1,*}

¹*Department of Mechanical Engineering and Materials Science Duke University Durham, NC 27708*

²*Department of Physics and Materials Research Institute Penn State University University Park, PA 16801*

**corresponding author, e-mail: stefano@duke.edu*

(Dated: November 7, 2018)

Lubricants can affect quasicrystalline coatings surfaces by modifying commensurability of the interfaces. We report results of the first computer simulation studies of physically adsorbed hydrocarbons on a quasicrystalline surface: methane, propane, and benzene on decagonal Al-Ni-Co. The grand canonical Monte Carlo method is employed, using novel Embedded Atom Method potentials generated from *ab initio* calculations, and standard hydrocarbon interactions. The resulting adsorption isotherms and calculated structures show the films' evolution from submonolayer to condensation. We discover the presence and absence of the 5- to 6-fold topological transition, for benzene and methane, respectively, in agreement with a previously formulated phenomenological rule based on adsorbate-substrate size mismatch.

Friction can become vanishingly small between incommensurate interfaces (superlubricity) [1, 2]. The aperiodic structure of quasicrystals surfaces makes them the ideal candidates for this phenomenon. Indeed, the special frictional properties of quasicrystals have been confirmed in a series of experiments using atomic force microscopy on single grain quasicrystals [3, 4, 5, 6, 7, 8]. Although its origin is not yet completely understood, the evidence suggests that poor coupling of phonons at the interfaces may play a major role [6, 7, 8]. In addition, there is also evidence that oxidation decreases the friction even further [4, 9]. In fact, even before these single crystal experiments were performed, experiments on quasicrystal coatings in air did show low-friction behavior [10], leading to applications involving moving machine parts and non-stick cookware [11].

Since the low friction of quasicrystals is clearly related to their structure, the interaction of the lubricant with the quasicrystal and the structure of the lubricating film is particularly important. In most applications involving machine parts, additional lubricant would be needed to address the frictional contributions of grain boundaries and asperities. Studies of metal and rare gas adsorption on quasicrystals indicate that both periodic and aperiodic structures can occur in thin films [12, 13, 14, 15, 16, 17]. However, little is known about the interaction of hydrocarbons with quasicrystal surfaces [5, 18, 19].

In the present manuscript, we explore the effect of structural and symmetry mismatches on the ordering of hydrocarbons by evaluating the nature of hydrocarbon adsorption (methane, propane, and benzene) on a quasicrystalline decagonal surface, namely, the tenfold surface of Al₇₃Ni₁₀Co₁₇. The simulations are performed using grand canonical Monte Carlo method (GCMC), with which we have extensive experience on smooth [20, 21, 22] and corrugated substrates [15, 16, 17, 23, 24, 25]. Using

the GCMC method, we compute the adsorption properties for specified thermodynamic conditions. We take a tetragonal unit cell, of side 5.12 nm, with a hard wall at 10 nm above the surface to confine the coexisting vapor phase without causing capillary condensation (sufficient to contain 25 layers of benzene). We assume periodic boundary conditions which, although sacrificing the accuracy of the long range QC structure, do not interfere with short-to-moderate length scales, representative of the hydrocarbon order. The substrate is reproduced with an 8-layer Al-Ni-Co slab, where the atom coordinates are derived from an experimental low-energy electron diffraction (LEED) study [26]. The inter-molecular interactions (adsorbate-adsorbate) are calculated as a sum of pair interactions between atoms. Buckingham potentials are used for methane [27, 28] and benzene [29, 30] while a Morse potential is employed for propane [31]. We have developed embedded-atom method (EAM) potentials [32] to model the many-body intra-molecular interactions, adsorbate-substrate (C-Al, C-Co, C-Ni, H-Al, H-Co, H-Ni), and substrate-substrate (Al-Al, Al-Co, Al-Ni, Co-Co, Co-Ni, Ni-Ni). The EAM embedding functions are taken as natural cubic splines using charge density functionals from Herman [33], while the EAM pair energies have Morse potential forms [34] with Haftel's mixing scheme [35], if necessary. The EAM potential parameters are fitted from *ab initio* energies calculated using the Vienna Ab-initio Simulation Package (VASP) [36] with exchange-correlation functionals as parameterized by Perdew, Burke, and Ernzerhof (PBE) [37] for the generalized gradient approximation (GGA), and projector augmented-wave (PAW) [38] pseudopotentials. The EAM potential parameters, fitted using the SIMPLEX method [39], are summarized in the EPAPS material [40]. Quasicrystal approximants (crystals having similar short-range order) are used to address the periodic boundary conditions required by the *ab initio* package: we use

$\text{Al}_{29}\text{Co}_4\text{Ni}_8$ (dB1), $\text{Al}_{17}\text{Co}_5\text{Ni}_3$ (dH1), and $\text{Al}_{34}\text{Co}_4\text{Ni}_{12}$ (dH2) [41]. Our calculations show that alkanes and benzene do not dissociate on such substrates, which do not undergo any considerable relaxation upon the adsorption of the molecules. Thus, as a first approximation, the substrate and the molecules can be considered rigid, although the molecules are allowed to explore all rotational degrees of freedom [42].

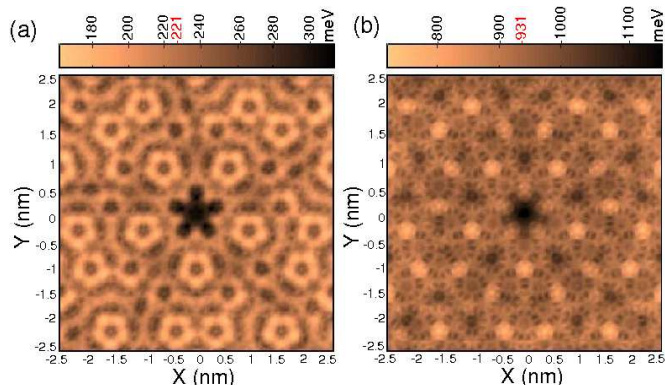


FIG. 1: (color online). Computed potential energies for (a) methane and (b) benzene on Al-Ni-Co, obtained by minimizing $V(x, y, z, \theta, \phi, \psi)$ of a single molecule with respect to (z, ψ, θ, ϕ) , variations. The average values are 221 meV/methane and 931 meV/benzene.

The adsorption potential of a single molecule, $V_{\min}(x, y)$, calculated as the maximum depth as a function of normal coordinate (z) and Euler angles (θ, ϕ, ψ) , is both deep and extremely corrugated. Figure 1 shows $V_{\min}(x, y)$ for methane and benzene: the dark spots indicate strong binding sites. The average adsorption energy is 221 meV/methane, 374 meV/propane, and 931 meV/benzene.

The symmetry of the adsorption potentials for methane and benzene reflect the pentagonal symmetry of the substrate, as illustrated in Fig. 1. Propane follows a similar trend as methane, with somewhat less corrugation due to its larger size. The most attractive adsorption positions for methane and propane [40] are located at the centers of pentagonal hollows having five Al atoms at the vertices. Conversely, the most attractive sites for benzene are the Al-centered pentagons with 3 Al and 2 Ni atoms at the vertices. These hollow and Al-centered pentagons alternate every 36° around the z axis.

By simulating the adsorption of a single molecule, a general trend is observed for the orientation of the adsorbant: the smaller the molecule, the more variation in the rotation of the ground state. Methane's ground state is highly degenerate, propane adsorbs with its axis forming a small angle with respect to the substrate (the angle varies from 0° to 10° depending on the adsorption site). Benzene adsorbs with its plane parallel to the substrate.

Figure 2 shows the computed adsorption isotherms

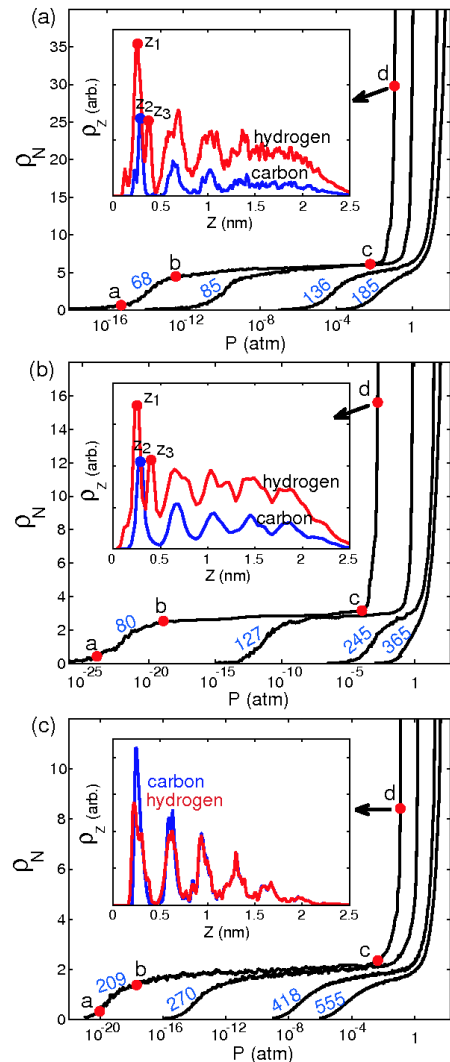


FIG. 2: (color online). Isothermal adsorption densities (ρ_N in molecules/ nm^2) of hydrocarbons on a decagonal Al-Ni-Co: (a) methane, (b) propane, and (c) benzene. The simulation temperatures are reported in blue (in Kelvin). The insets represent the densities along the z direction at P corresponding to points “d”.

ρ_N (densities in molecules/ nm^2) at different temperatures for methane ($T=68, 85, 136, 185$ K), propane ($T=80, 127, 245, 365$ K), and benzene ($T=209, 270, 418, 555$ K) as functions of pressure P . The plotted quantities are the thermodynamic excess coverages (differences between the total number of molecules and the number that would be present if the cell were filled with uniform vapor). The substrate is very attractive (Fig. 1) hence the hydrocarbons experience complete wetting up to the highest temperature close to the critical temperature. At low temperatures, the formation of the first layers is evident from the first step in each plot (the most left isotherms). The formation of further layers is not clearly observed in contrast with the observations for noble gases

[15, 16, 17, 24]. Nevertheless, layering in the adsorbed film is revealed by the insets of Fig. 2 showing the adsorption densities along the z direction at the pressures corresponding to points “d” of the lowest temperature isotherms. The relative positions of z_1 , z_2 , and z_3 indicate that methane adsorbs mostly with three hydrogens anchored to the substrate, while propane adsorbs mostly with five hydrogens near the substrate (two from each end and one from the middle segment).

In the submonolayer regime (point “a” in Figure 2(a)), methane adsorbs preferentially at the strong binding sites. By increasing P , a methane monolayer forms with pentagonal ordering commensurate with the substrate (point “c” in Figure 2(a)). Similar configurations are observed at all studied temperatures. An example of such ordering is illustrated in Fig. 3(a) at $T=68\text{K}$: the density profile $\rho(x, y)$ and the Fourier transform FT_{cm} of the density of the center of mass confirm pentagonal ordering (10 discrete spots representing 5-fold axes in FT_{cm}). Similar plots for propane at 80 K and benzene at 209 K are shown in Figure 3 (b) and (c), respectively. At all simulated temperatures, benzene has 6-fold order as indicated by its FT_{cm} characteristic of triangular lattice. Unlike methane and benzene, which adsorb in a well-defined structure, propane forms a poorly-ordered 5-fold arrangement (clusters of molecules which form pentagons can be seen in the EPAPS material [40]). The FT_{cm} indicates a distortion involving a compression along one direction. This is due to the interplay between the linear form of propane molecule and the quasicrystal structure. Figure 4 shows a histogram of the orientations of the propane’s axis projected on the xy -plane (panel (a)) and the xz -plane (panel (b)), corresponding to the density plot in Figure 3(b). Indeed, propane adsorbs with its axis parallel with the substrate (up to 10°) and preferentially oriented along y -axis.

Figure 5(a) illustrates a superposition of the methane monolayer at 85 K and the top layer of substrate atoms. Methane molecules are present in every hollow pentagon defined by five Al atoms. These pentagons, corresponding to the dominant binding sites and depicted as dark spots in Fig. 1(a), are responsible of stabilizing the quasicrystalline structure of the methane monolayer. A similar plot for benzene at 209 K is given in Figure 5(b). A domain having 6-fold order can be observed in the left part of the figure. Dotted circles corresponding to the benzene molecules, along with two red lines illustrate the orientation of this domain, which makes an angle of 18° from the y -axis. Thus, the benzene lattice is oriented along a symmetry direction of the quasicrystal, as observed previously for the Xe monolayer.

Previously, by studying adsorbed monolayer of rare gases [16, 17], we found that the crucial parameter in de-

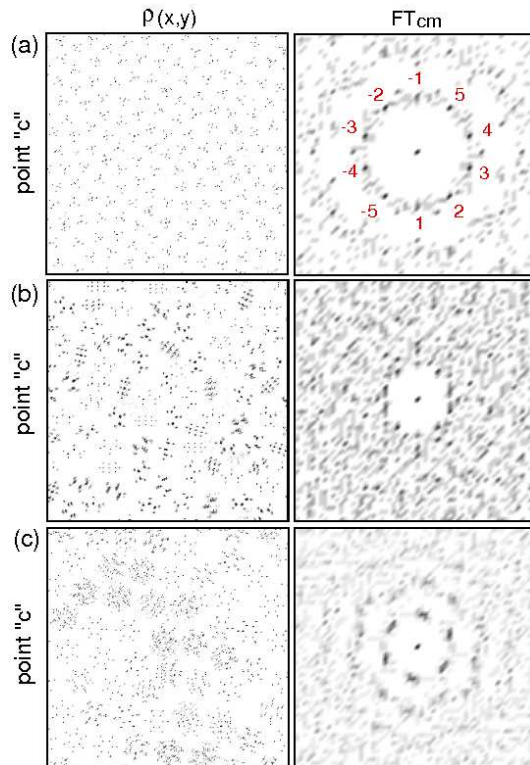


FIG. 3: Monolayer density profiles $\rho(x, y)$ and Fourier transforms of the density of the center of mass FT_{cm} for: (a) methane at 68 K (point “c” in Figure 2(a)), (b) propane at 80 K (point “c” in Figure 2(b)), and (c) benzene at 209 K (point “c” in Figure 2(c)) adsorbed on decagonal Al-Ni-Co.

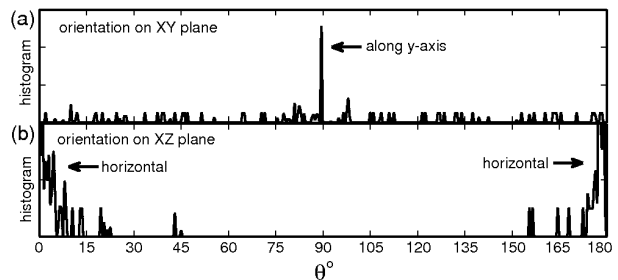


FIG. 4: Histogram of orientation of propane’s axis on (a) XY plane and (b) XZ plane at monolayer coverage at 80 K adsorbed on decagonal Al-Ni-Co. The corresponding density plot is depicted in Figure 3(b).

termining the overlayer structure is the relative size mismatch between adsorbate and substrate’s characteristic length. The mismatch is defined as $\delta_m \equiv (d_r - \lambda_r)/\lambda_r$ where d_r is the distance between rows in a 2D close-packed arrangement of adsorbates [17, 43], and $\lambda_r = 0.381$ nm is the quasicrystal’s characteristic length [14]. Thus, δ_m measures the relative mismatch between an adsorbed $\{111\}$ closed packed plane of adsorbates and the QC surface. The proposed rule states that the ordering transition exists if and only if $\delta_m > 0$ [17]. For methane, by starting from the lattice parameter of the cubic cell

[44, 45], we have $\delta_m(\text{CH}_3) \sim -0.055$. For benzene, by using d_r obtained from the simulation of the 6-fold phase (using a flat substrate with the well depth of 931 meV), we get $\delta_m(\text{C}_6\text{H}_6) \sim 0.617$. Both methane and benzene satisfy the mismatch rule extending its applicability (the transition can not be defined for propane since it does not form pentagonal or triangular arrangements).

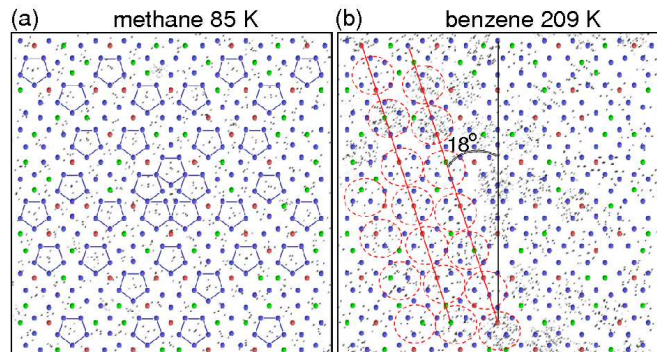


FIG. 5: (color online). (a) methane monolayer at 85 K (b) benzene monolayer at 209 K adsorbed on decagonal Al-Ni-Co. Top layer of substrate atoms are plotted in blue (Al), green (Ni), and red (Co).

TABLE I: Summary of adsorbed rare gases and selected hydrocarbons undergoing (or not) the commensurate \rightarrow incommensurate transition on-Al-Ni-Co. iNe, iXe, and dXe are inflated/deflated noble gases [17]. Triangles and pentagons indicate triangular lattice and fivefold structure, respectively.

	δ_m	transition	monolayer
methane	-0.055	No	\diamond
benzene	0.617	Yes	\triangle
Xe [15, 16]	0.016	Yes	\triangle
Ne [17]	-0.311	No	$\triangle + \diamond$
Ar [17]	-0.158	No	$\triangle + \diamond$
Kr [17]	-0.108	No	$\triangle + \diamond$
iNe ⁽¹⁾ [17]	0.016	Yes	\triangle
dXe ⁽¹⁾ , dXe ⁽²⁾ [17]	-0.311, -0.034	No	$\triangle + \diamond$
iXe ⁽¹⁾ , iXe ⁽²⁾ [17]	0.363, 0.672	Yes	\triangle

Table I summarizes the results obtained for all hydrocarbons and rare gases that we have studied so far. When the transition is not present, the monolayer does not form a structure having long-range periodic order. From the point of view of the potential for superlubricity, all of the gases that are smaller than Xe do not form periodic films. In addition, the linear molecule propane, which is larger than Xe, does not. This suggests that the shape as well as the size is an important factor in the ordering, and it may bode well for the use of linear hydrocarbons as lubricants on quasicrystalline films.

Research supported by NSF (DMR-0505160, DMR-0639822) and ACS (#PRF-45814-G5). We thank the

Teragrid Partnership (Texas Advanced Computing Center, TACC) for computational support (MCA-07S005).

- [1] M. Hirano and K. Shinjo, Phys. Rev. B **41**, 11837 (1990).
- [2] M. Dienwiebel *et al.*, Phys. Rev. Lett. **92**, 126101 (2004).
- [3] J. Y. Park *et al.*, Tribology Letters **17**, 629-636 (2004).
- [4] J. Y. Park *et al.*, Science **309**, 1354-1356 (2005).
- [5] J. Y. Park *et al.*, Phys. Rev. B **71**, 144203 (2005).
- [6] J. Y. Park *et al.*, Phys. Rev. B **74**, 024203 (2006).
- [7] J. Y. Park *et al.*, Phil. Mag. **86**, 945-950 (2006)
- [8] J. Y. Park *et al.*, J. Phys.: Condensed Matt. **20**, 314012 (2008)
- [9] J. M. Dubois *et al.*, Phil. Mag. **86**, 797 (2006)
- [10] J. M. Dubois, S. S. Kang, and J. Von Stebut J. Mat. Sci. Lett. **10**, 537-541 (1991).
- [11] Dubois, J.M. 2003, *Useful Quasicrystals* (Singapore: World Scientific Publishing Co.).
- [12] V. Fournée and P. A. Thiel, J. Phys. D: Appl. Phys. **38**, R83 (2005).
- [13] H. R. Sharma, M. Shimoda, and A. P. Tsai, Advances in Physics **56**, 403-464 (2007).
- [14] N. Ferralis *et al.*, Phys. Rev. B **69**, 075410 (2004).
- [15] S. Curtarolo *et al.*, Phys. Rev. Lett. **95**, 136104 (2005).
- [16] W. Setyawan *et al.*, Phys. Rev. B **74**, 125425 (2006).
- [17] W. Setyawan *et al.*, J. Phys.: Condens. Matter **19**, 016007 (2007).
- [18] J. T. Hoeft *et al.*, Philos. Mag. **86**, 869 (2006).
- [19] R. McGrath *et al.*, J. Alloys and Compounds **342**, 432 (1992).
- [20] F. Ancilotto *et al.*, Phys. Rev. Lett. **87**, 206103 (2001).
- [21] S. Curtarolo *et al.*, Phys. Rev. E **59**, 4402 (1999).
- [22] M. J. Bojan *et al.*, Phys. Rev. E **59**, 864-873, (1999).
- [23] S. Curtarolo *et al.*, Phys. Rev. E **59**, 4402-4407, (1999).
- [24] R. D. Diehl *et al.*, Phil. Mag. **87**, 2973 (2007).
- [25] R. D. Diehl, W. Setyawan, and S. Curtarolo, J. Phys. Cond. Matt. **20**, 314007 (2008).
- [26] N. Ferralis *et al.*, Phys. Rev. B **69**, 153404 (2004).
- [27] S. Tsuzuki, T. Uchimaru, and K. Tanabe, J. Mol. Struct. **280**, 273 (1993).
- [28] S. Tsuzuki *et al.*, J. Phys. Chem. **98**, 1830 (1994).
- [29] S. Califano, R. Righini, and S.H. Walmsley, Chem. Phys. Lett. **64**, 491 (1979).
- [30] R. Chelli *et al.*, Phys. Chem. Chem. Phys. **3**, 2803 (2001).
- [31] J.-P. Jalkanen *et al.*, J. Chem. Phys. **116**, 1303 (2002).
- [32] M. S. Daw and M. L. Baskes, Phys. Rev. Lett. **50**, 1285 (1983).
- [33] A. Herman, Int. J. Nanotech. **2**, 215 (2005).
- [34] P. M. Morse, Phys. Rev. B **34**, 57 (1929).
- [35] M. I. Haftel, Phys. Rev. B **48**, 2611 (1993).
- [36] G. Kresse and J. Hafner, Phys. Rev. B **47**, 558 (1993).
- [37] J. P. Perdew, K. Burke, and M. Ernzerhof, Phys. Rev. Lett. **77**, 3865 (1996).
- [38] P. E. Blöchl, Phys. Rev. B **50**, 17953 (1994).
- [39] J. A. Nelder and R. Mead, The Computer Journal **7**, 308 (1965).
- [40] See EPAPS Document No. XXXXXX for the functionals and the fitted parameters of the EAM potentials for hydrocarbons on Al-Ni-Co, additional adsorption potential energy surface, and density profiles. This document can be reached via a direct link in the online article's HTML reference section or via the EPAPS homepage (<http://www.aip.org/pubservs/epaps.html>).
- [41] Database of alloys <http://alloy.phys.cmu.edu/>
- [42] Even though the substrate is rigid, it experiences different charge density in different GCMC configurations, therefore the embedding energy needs to be updated in each step.
- [43] For adsorbates described by LJ interactions $d_r = k \cdot \sigma_{gg}$, where $k = 0.944$ is the distance between rows in a close-packed plane of a bulk LJ gas with $\sigma = 1$ at $T = 0$ K [46], and σ_{gg} is the

- LJ size parameter of the gas-gas potential.
- [44] H. H. Mooy, *Nature* **127**, 707 (1931)
- [45] H. M. James and T. A. Keenan, *J. Chem. Phys.* **31**, 12 (1959).
- [46] L. W. Bruch, P. I. Cohen, and M. B. Webb, *Surf. Sci.* **59**, 1 (1976).